A study of completely decomposed volcanic rock with a transitional mode of behaviour

OKEWALE Ismail Adeniyi[1] and **COOP** Matthew Richard[2]

Authors Affiliations

[1]Federal University of Technology Akure, Nigeria

Formerly City University of Hong Kong, Tat Chee Avenue, Hong Kong

iaokewale@futa.edu.ng (corresponding author)

ORCID: 0000-0003-1115-7479

[2] Professor of Geotechnical Engineering

University College London, UK

Formerly City University of Hong Kong, Tat Chee Avenue, Hong Kong

m.coop@ucl.ac.uk

Abstract

A transitional mode of behaviour is seen in some soils where the specific volumes of samples do not converge to the same values at the same stress state within the ranges of strains that can be achieved in laboratory tests so there are no unique normal compression or critical state lines. This type of behaviour has been found in different soils but not previously in soils resulting from decomposed igneous rocks. In order to investigate the possibility of transitional mode of behaviour in a decomposed volcanic rock, an extensive series of one-dimensional compression and triaxial tests were conducted on samples in reconstituted and intact states. The important features of transitional mode of behaviour in soils have been identified, that is, the presence of non-unique and parallel normal compression and critical state lines. The behaviour of the soil is therefore dependent on the initial specific volume. The degree of transitional behaviour is strong, particularly in the reconstituted samples but it is less clearly identified in the intact samples due to the small range of initial specific volumes available. These observations indicate that the transitional mode of behaviour, previously seen in sedimentary soils and artificial soil mixtures can be extended to some weathered igneous rocks. Determining the effects of structure is difficult due to the non-unique intrinsic properties but nevertheless, the effects of structure have been identified and discussed.

Keywords: Transitional behaviour, igneous rocks, decomposed volcanics, fabric, natural structure

Introduction

Many soils have been found to exhibit a transitional mode of behaviour, which are characterized by non-unique normal compression lines (NCL) and critical state lines (CSL) in the specific volume (v) or void ratio (e): log vertical effective stress or mean effective stress plane (v/e: $\log\sigma'_v$ or v/e: lnp') (e.g., Ponzoni et al. 2017; Shipton and Coop 2012; Ferreira and Bica 2006; Martins et al. 2001). The major feature of transitional behaviour is that samples at different initial specific volumes do not converge to unique values at a given stress in either compression or shearing. This may be possibly due to the soils still preserving some features of the initial differences in the fabric even after compression to high stresses or shearing to larger strains (e.g., Todisco et al. 2018). This behaviour has been found in soils with natural sedimentary origins soils (e.g., Xu and Coop 2017; Ponzoni et al. 2014; Nocilla et al. 2006), one weathered sedimentary soil (Ferreira and Bica 2006) and artificial laboratory mixtures of soils (e.g., Shipton and Coop 2012; Shipton and Coop 2015; Shipton et al. 2006), but has not previously been seen in soils of weathered igneous origin.

Although many transitional soils are gap graded in nature, the behaviour has also been found in well graded silty clays (Nocilla et al. 2006) and well graded sands (Todisco et al. 2018). The factors responsible for this mode of behaviour have not been fully understood but it may be that strong fabrics that are difficult to break down in simple compression and shearing might be responsible. It was on this premise that Todisco et al. (2018) investigated some elements of fabrics at a microscale for transitional soils using mercury intrusion porosimetry (MIP), examining pore size distributions (PSD) and their evolution in compression and shearing. They established that robust fabrics which could not be broken down during conventional testing can be responsible for the lack of convergence.

However, investigations into the transitional behaviour in well-graded weathered geomaterials are very scarce compared to those in other materials and to the best of our knowledge, there has never been an investigation on transitional behaviour in decomposed volcanics. The work described in this paper presents the mechanics for a transitional mode of behaviour in completely decomposed volcanic rock in intact and reconstituted states.

Materials used

The samples tested were completely decomposed volcanic rock from Hong Kong, locally called tuffs and belonging to Tai Mo Shan formation of the Tsuen Wan volcanic group, which is coarse-grained. The sample was classified based on the international six grade classification (e.g., ISRM 2007) upon which local classifications for Hong Kong geomaterials are based (e.g., GEO 1988). The samples were taken as Mazier rotary cores from the New Territories in northern Hong Kong, under the supervision of the Geotechnical Engineering Office of Hong Kong. The samples were retrieved from 4-5 m depth and the sample description is shown in Table 1. Figure 1 presents the particle size distribution of the sample determined by a combination of wet sieving and sedimentation. Okewale (2017) and Okewale and Coop (2017) tested a much wider variety of similar decomposed volcanics from other Hong Kong formations, none of which had a transitional behaviour. Data for that completely decomposed volcanic (CDV) from Okewale and Coop (2017) that was most similar to the soil studied here will be shown in this paper for comparison, and its grading is also given in Figure 1.

Table 1. Sample description and index properties

Formation	Depth (m)	Grading	d_{50} (mm)	c_u	Clay fraction (%)	Silt fraction (%)	Liquid limit (%)	Plastic limit (%)	Plasticity Index (%)
TMSF	4-5	Coarse	0.01	150	28	30.7	35.5	26.1	9.4

TMSF Tai Mo Shan Formation, d_{50} mean particle size, c_u coefficient of uniformity

The soil is well graded and can be classified as sandy silt. The mean particle size (d_{50}) is 0.01mm and modified coefficient of uniformity ($C_u = d_{70}/d_{20}$) is 150, which also confirms the well-graded nature of the sample similar to other CDVs (e.g., Okewale and Coop 2017, 2018b; Okewale 2019c, 2020; Okewale and Grobler 2020). The soil comprises 28% clay fraction and a silt-sized fraction of 30.8%. The liquid limit and plastic limit of the samples are 35.5% and 26.1%, giving a plasticity index of 9.4%. The sample can be classified as silt with low plasticity.

Figure 2 shows the microstructure of the intact samples in the horizontal and vertical plane. The fabrics are characterised by agglomerations of flat particles forming continuous clusters with very few intra-cluster voids. The intact fabric is heterogeneous and with no perceivable particle orientation in both planes. The microstructure of the reconstituted sample in horizontal and vertical plane is presented in Figure 3 and is again characterised by agglomerations of flat particles, but which appear well arranged and more compact with few voids, the agglomerates being in a continuous matrix.

The samples comprise about 37% quartz, 20% feldspars, 30% clay minerals and 13% of other minerals (Table 2). The clay minerals result basically from feldspars and biotite which are the primary minerals of the parent rock together with quartz. The details of the chemical composition are shown in Table 3. Again, a high percentage of silica indicates the presence of quartz and a low proportion of alkaline and alkaline earth cation is an indication of an alteration of feldspars in the sample. The relatively high proportion of alumina is an indication of the presence of clay minerals and sesquioxides resulting directly from biotite.

Table 2. Mineralogy from XRD analysis

Minerals (%)			
Quartz	Feldspars	Clays	Others
37	20	30	13

Table 3. Chemical compositions from XRF analysis

Chemical compositions (%)							
Na_2O	CaO	MgO	Al_2O_3	SiO_2	K_2O	TiO_2	Fe_2O_3
1.44	0.27	0.06	19.42	62.14	2.23	1.54	12.90

Methodology

A Philips XL30 FEG Environmental Scanning Electron Microscope (ESEM) was used to study the microstructure of the intact and reconstituted samples. In order for the samples to give a true reflection of the fabric, broken surfaces rather than cut surfaces were used and the micrographs are studied in the vertical and horizontal plane. A Bruker X-ray diffractometer was used to investigate the bulk mineralogy of the sample in powder form. The chemical composition of the sample was studied using a Shimadzu EDX-720 Energy Dispersive X-ray Fluorescence Spectrometer (XRF), again analysing the sample in a powder form.

Oedometer tests were used to investigate the behaviour of the sample in one-dimensional compression. Fixed base rings of 50mm diameter and 20mm height were used for the reconstituted samples and a stress of up to 7 MPa was achieved. To reach higher stresses while reducing wall friction, a floating ring type of 30mm diameter was used for the intact samples for stresses of up to about 20 MPa. The intact samples were trimmed directly into the confining ring on a hand lathe very carefully in order to minimize the disturbance to the sample. A small downward pressure was applied to the sample, excavating the sample slightly ahead of the ring. The reconstituted samples for the oedometer tests were prepared by adding varying amounts of distilled water to create slurry samples of different initial densities that were placed directly into the ring.

Several methods were used to calculate the initial specific volumes. The measurements were carried out with great care because of the importance of the accuracy of the specific volume in establishing whether there was really non-convergence of compression paths or non-uniqueness of the critical state lines. The initial v was calculated from the initial dimensions and initial water contents and also back calculated from final dimensions and final water contents, using several methods as outlined in detail by Rocchi and Coop (2014) and used by several studies (e.g., Rocchi and Coop 2016; Okewale 2019a, 2019b, 2019c). The accuracy of the specific volumes was estimated by taking the maximum difference between any individual value of v and the mean from the various methods giving an estimated accuracy for the oedometer tests for both the reconstituted and intact samples of ±0.02.

The shearing behaviour was investigated using several triaxial apparatus, one of conventional design, one an Imperial College (IC) stress path system and one a GDS stress path cell. The conventional triaxial apparatus and the IC cell could apply a cell pressure of up to 750 kPa and they were used for the reconstituted samples. A cell pressure of up to 2 MPa was applied by GDS cell and it was used for the intact samples.

The samples were of different diameters but a height to diameter ratio of 2:1 was used in each. The Mazier sample tube was 75mm diameter and intact samples for the triaxial tests were prepared by cutting the tube to the required length using a diamond rotary saw while the sample was still in the tube. A machine end cutter was used to cut several slots along the length of the tube while providing the support to the sample. The parts of the tube between the slots were then carefully removed from the sample and the perimeter of the sample was dressed. However, only two intact triaxial samples were tested due to highly heterogeneous nature of the soil, the limited soil availability and the difficulty involved in reducing the samples to sample smaller sizes.

The reconstituted samples for the triaxial tests were prepared again as slurries of various water contents which were then either compressed in a consolidometer tube prior to placing on the platen or prepared directly on the platen by pouring the slurry inside a membrane within a mould. The average estimated accuracy of the values of v for the triaxial tests for both the reconstituted and intact samples is ±0.010, slightly better than the oedometers because of the larger sample sizes (Ponzoni et al. 2014). The estimated accuracies are similar to other studies investigating transitional behaviour in soils, using similar methods (e.g., Shipton and Coop 2012; Nocilla et al. 2006).

Results and discussions

Compression behaviour

The behaviour in compression was studied by carrying out many oedometer tests and the design of the testing programme was to determine whether there was transitional behaviour in the reconstituted and intact samples. Also, the effect of structure was established by comparing the reconstituted and intact samples. In order to determine the presence of a transitional mode of behaviour, a wide range of initial specific volumes is required, so the samples were prepared to achieve different initial densities. Figure 4 presents the compression data for the reconstituted samples prepared at different initial states. The details of the oedometer tests are given in Table 4.

At higher stresses, the compression paths appear parallel and there is almost no convergence, with a spacing between the lines that is much greater than the estimated average accuracy for v of ±0.02, indicating that the non-convergence of the paths is not the result of error in the measurement of v. This is a clear transitional mode of behaviour in compression because it will be impossible to reach a unique normal compression line before the compression paths must tend towards a horizontal asymptote at v=1 at a very high stress.

Table 4. Details of oedometer tests

Sample/test type	w_i	v_i	$\sigma_{v\ max}$ (kPa)
RO1	0.275	1.787	7145
RO2	0.499	2.304	7155
RO3	0.419	2.093	7152
RO4	0.447	2.192	7124
RO5	0.422	2.144	7144
RO6	0.306	2.319	7147
RO7	0.409	2.137	7147
RO8	0.420	2.126	7141
RO9	0.418	2.126	7152
RO10	0.444	2.002	7158
RO11	0.407	2.019	7144
RO12	0.470	2.254	7144
RO13	0.459	2.152	7139
RO14	0.323	1.907	7138
RO15	0.323	1.893	7151
RO16	0.359	2.008	7165
RO17	0.362	2.002	7171
RO18	0.390	2.017	7171
RO19	0.530	2.390	7165
IO1	0.320	1.991	19854
IO2	0.273	1.992	19854
IO3	0.273	1.839	19854
IO4	0.302	1.861	19854
IO5	0.327	1.858	19854

R reconstituted, I intact, w_i initial/ in-situ water content, v_i initial specific volume, $\sigma_{v\ max}$ maximum vertical stress.

As shown in Figure 3, the continuous clusters from the agglomeration of particles float in a matrix, which perhaps results in a strong form of fabric which is robust and cannot be broken down in compression, thereby leading to non-convergent behaviour of this soil. For the purpose of comparison, the oedometer tests on the similar reconstituted CDV samples studied by Okewale and Coop (2017), of which the grading curve is shown in Figure 1 are presented in Figure 5. A fully convergent behaviour was found with a unique intrinsic normal compression line (NCL*), indicating that the initial differences in the specific volumes have been erased. This conventional convergent behaviour might be attributed to fabric in which the clusters are not continuous and are not floating in matrix as seen in Figure 6(a), so while the gradings of the two soils are similar and similar reconstitution methods have been used, it is the very different fabrics that are responsible for the different modes of behaviour.

The transitional behaviour cannot be attributed to the repeatability of the tests because other soils investigated by Okewale and Coop (2017) were prepared to different initial densities similar to the method here and the compression curves converged, in contrast to what is seen in this study. Also, the mineralogy of the sample used in this work is not significantly different from those of Okewale and Coop (2017) and so that is unlikely to be the cause. The soils comprised basically quartz, feldspars, clays and other accessory minerals, although in different proportions. The transitional behaviour can instead be linked to the heterogeneous fabric, which is characterised by continuous clusters as observed in the SEM micrographs. However, SEM micrographs have limited and qualitative use in determining where the seat of fabric will lie. On the other hand, mercury intrusion porosimetry (MIP) could be a useful quantitative tool, as used by Todisco et al. (2018) to investigate fabrics in transitional soils, although on soils with much simpler mineralologies and gradings. Furthermore, it has been suggested that transitional behaviour in soil can be linked to fabric heterogeneity rather than anisotropy of fabric (Shipton and Coop 2015; Todisco et al. 2018) and the SEM images do reveal a strong heterogeneity. While a transitional mode of behaviour has been brought about in some studies by simply varying the grading (e.g., Shipton and Coop 2012), this is clearly not the case for this behaviour in soils resulting from decomposed volcanic rocks.

Figure 7 shows the compression data for the intact samples. The compression paths seem again not to converge, similar to those of the reconstituted samples. Considering the accuracy of initial v, the offsets between the compression curves at the end of the tests again indicate that the intact samples exhibit a transitional mode of behaviour. The compression data of the intact CDV samples studied by Okewale and Coop (2017) are presented in Figure 8. After yielding, the compression curves converge, indicating a non-transitional mode of behaviour similar to the behaviour in the reconstituted state which can also be linked to fabric that is dominated by less continuous clusters with large inter and intra cluster voids (Fig. 6(b)). However, it is difficult to investigate transitional behaviour in the intact samples because they are created naturally, so the initial v cannot be chosen and there is therefore a limited range of values available. This was the reason for so many reconstituted samples being tested in this research.

In order to quantify the degree of transitional behaviour in compression, a parameter m, based on oedometer data proposed by Ponzoni et al. (2014) was employed. The m value was calculated by plotting the initial specific volume (taken at 20kPa, v_{20}) against the specific volume at 7000kPa (v_{7000}), being the approximate maximum stress reached in the tests presented in this paper. Ponzoni et al. (2014) used v_{6000} because the highest stress reached in their test was 6000kPa. It is believed that the effect on m would be very small (Xu and Coop 2017). The value of m can range between 0 (fully non-transitional) and 1 (fully transitional).

Figure 9 presents the m values for the reconstituted and intact samples. The line of best fit is for the reconstituted samples only. There is clear positive gradient for the reconstituted samples which is an indication of non-convergence of compression paths with an m value of 0.39. Based on the m value of the reconstituted samples, the degree of transitional behaviour can be classified as medium.

The m value cannot be estimated for the intact samples due to difficulties discussed above. It has previously been found that the degree of lack of convergence is higher in intact samples than in reconstituted samples for some soils (e.g., Ponzoni et al. 2014). The intact samples plot above the reconstituted samples, indicating the effects of a natural structure in addition to that which must cause the transitional behaviour.

Ferreira and Bica (2006) pointed out how difficult it was to quantify the effects of structure in soils without unique intrinsic properties, but nevertheless, an attempt is made here because significant effects of structure have been highlighted in similar soils with no transitional mode of behaviour (Okewale and Coop 2017, 2018a; Rocchi et al. 2015). These data may be normalised using void index $I_v = (e-e^*_{100})/(e^*_{100}-e^*_{1000})$, where e^*_{100} and e^*_{1000} are the void ratios on the intrinsic compression line, ICL at 100 and 1000kPa, as proposed by Burland (1990) (Fig.10). Here the ICL was found to be straight as indicated on Figure 10. The ICLs were taken at higher stresses where the paths appear to be parallel. The ICLs were determined for reconstituted samples with similar specific volumes to those of the intact samples at the initial stress of 20kPa and these were used for the quantification of the effects of structure. Because of the different ICLs, while a uniform gradient was used for each sample Figure 9 was used to calculate an intercept of the ICL for the value of v of each intact sample, i.e. each intact sample has its own ICL.

The compression paths of the intact samples cross the ICL of the reconstituted samples and then converge slowly towards it. States outside the ICL are reached and a significant effect of structure is identified. The samples yield at low stresses, but the convergence of the compression paths towards the ICL is variable and even at the highest possible stresses, some samples do not reach it. This shows that some samples have not been completely destructured at the end of the test, or at least destructured to a similar state to the equivalent reconstituted sample. The compression curves of the non-transitional CDV samples studied by Okewale and Coop (2017) cross the ICL at very high vertical stresses due to low initial specific volumes and seem to show a weaker effect of structure. A slower convergence of compression paths to the ICL in Figure 10 may be linked to the same dominance of fabric in the soil which might give rise to the transitional behaviour.

Shearing behaviour

Figures 11 and 12 present the stress-strain behaviour of the samples in undrained and drained loading respectively. Details of the tests are given in Table 5. Grey lines are used for the reconstituted samples and black lines are used for the intact samples. The labels indicate the type of sample (reconstituted/intact) with the first letter, followed by mean effective stress p' prior to shearing, then type of loading (drained/undrained) and finally, the number of the test if there are more than one for the same mean effective stress. The changes in pore pressure (Δu) have been normalised by mean effective stress prior to shearing (p_o') for the undrained tests (Fig. 11b). The stress-strain behaviour depends on both the stress level and type of loading but generally the deviatoric stress rises monotonically with axial strain to a critical state (Figs. 11a and 12a), similar to the study of Okewale and Coop (2017) on samples of other formations. In some samples, pore pressure changes increase with axial strain to a peak and then slowly decrease until the critical state is reached. The pore pressure changes and volumetric strains are positive and the behaviour of the samples is contractive and strain hardening (Figs. 11b and 12b).

Figure 13 presents the stress paths and critical states for the samples. The stress paths are shown for only reconstituted samples in undrained loading. Only the critical states are shown for the reconstituted samples in drained loading and intact samples. There is a unique critical state line (CSL) in the stress plane with a gradient M of 1.46.

Table 5. Details of triaxial tests

Sample/test type	v_i	p'_c (kPa)	v_c	End of shearing		
				q_{cs} (kPa)	p'_{cs} (kPa)	v_f
R50U	1.940	48	1.927	110	73	1.927
R50D	1.656	50	1.622	148	100	1.612
R100U1	1.800	100	1.770	189	130	1.770
R100U2	2.000	100	1.908	134	85	1.908
R100D1	1.759	100	1.712	260	186	1.691
R100D2	1.875	100	1.822	245	181	1.762
R100D3	2.006	100	1.902	236	180	1.838
R200U1	1.649	199	1.574	311	217	1.574
R200U2	1.721	199	1.631	189	150	1.631
R200U3	1.983	199	1.832	385	255	1.832
R200D	1.673	198	1.609	630	407	1.607
R220D	1.839	219	1.760	630	430	1.697
R250D1	1.625	249	1.537	531	425	1.495
R250D2	1.633	248	1.529	602	448	1.461
R270U	1.805	269	1.693	338	249	1.693
R300U1	1.659	299	1.539	435	315	1.539
R300U2	2.046	298	1.868	577	398	1.868
R300D1	1.875	299	1.747	762	551	1.685
R300D2	1.271	299	1.182	800	564	1.137
R350D	1.836	349	1.668	995	679	1.595
R400U	1.781	399	1.631	642	440	1.631
R400D	1.774	399	1.616	1239	809	1.538
R450U	2.044	450	1.839	507	409	1.839
R500U	1.886	497	1.691	495	346	1.691
R500D	1.768	500	1.624	1750	1081	1.517

I100U	1.842	98	1.830	207	138	1.830
I500D	1.870	500	1.747	1174	890	1.612

R reconstituted, I intact, v_i initial specific volume, p'_c mean effective stress prior to shearing, v_c specific volume before shearing, q_{cs} deviatoric stress at critical state, p'_{cs} mean effective stress at critical state, v_f final specific volume.

Figure 14 shows the evolution of stress ratios for the samples. Again, grey lines are used for the reconstituted samples and the black lines for the intact samples. With a little scatter, this also confirms the unique critical state line gradient M. The M value is within the range 1.25-1.52 found for similar saprolitic soils (e.g., Okewale and Coop 2017; Rocchi and Coop 2015). This behaviour is in agreement with other studies (e.g., Ferreira and Bica 2006; Nocilla et al. 2006) showing that non-uniqueness of the critical states in the volumetric plane is not connected with non-uniqueness in terms of strength.

Figures (15) and (16) show the non-convergence of states in drained and undrained loading for the reconstituted samples. It is expected that if a unique critical state line exists in the v:lnp' plane, drained tests at the same p' but different initial specific volumes v should converge to a unique v at the critical state. Also, undrained tests at the same specific volume but different initial p' should converge to unique p'. These do not happen and the tendency to converge is very small because the initial differences in the p' or v tend to remain throughout shearing, similar to what was found for other transitional soils (Shipton and Coop 2015; Ponzoni et al. 2014).

The behaviour of the reconstituted and intact samples in the volumetric plane is shown in Figure 17. The isotropic compression and shearing paths, as well as the critical states for all the tests are shown. The arrow indicates a test that was still strain softening when terminated. Within the range of stresses investigated, straight CSLs were chosen and in estimating the CSLs, a unique value of the slope λ was assumed for simplicity. Different critical state lines are found for the reconstituted samples and several estimated lines for samples with similar initial specific volumes are given. The locations of the CSLs in the volumetric plane are therefore influenced by the initial specific volumes of the samples. This again shows transitional behaviour in this soil, similar to other transitional soils. The behaviour is also clearly in contrast to the CDV samples investigated by Okewale and Coop (2017) which had a unique CSL that plots well above any of the parallel CSLs found here (Fig. 17a). Because there are too few data for the intact samples, a conclusion cannot be made whether there will be a unique CSL for these (Fig. 17b).

To quantity transitional behaviour in shearing, a parameter P proposed by Ponzoni et al. (2014) based on the locations of CSLs was employed. The value of P was calculated by plotting the initial specific volume (v_o) before consolidation against the projected intercept of the critical state line (Γ) at 1kPa. Similar to the quantification of transitional behaviour in compression, the gradient of the relationship is defined as parameter P and the value must range between 0 (fully non-transitional) and 1 (fully transitional). Figure 18 presents the calculation of parameter P. The destructuration of the intact samples during shearing seems to be more than that in compression allowing the data for the intact samples to plot close to the reconstituted data line. The arrow points to the data point for the strain softening sample which has been included in the regression. The P value of 0.84 is found for the reconstituted samples and this is significantly higher than m value for the reconstituted samples. This indicates that there has been less convergence of volume in shearing than in compression, which is a feature also found by other researchers (e.g., Ponzoni et al. 2014) and has been attributed to the much higher stresses reached in the oedometer tests compared to the triaxial tests.

The degree of transitional behaviour as quantified by P for the reconstituted decomposed volcanic rocks is found to be slightly higher than the values reported for sediments of the Venice lagoon by Ponzoni et al. (2014). Again, due to there being too few data and a limited range of initial v, it is difficult to quantify any transitional behaviour for the intact samples. However, transitional behaviour has been found by others to be higher in intact than in reconstituted samples for some silty soils (e.g., Ponzoni et al. 2014). The fact that on Figure 17 the critical states of the intact and reconstituted samples are similar, while the volumetric states remained distinctly different in compression (Fig. 9) does highlight that those aspects of structure that give the underlying transitional behaviour of the reconstituted soil and those aspects that give rise to differences between the intact and reconstituted soil are affected very differently by compression and shear.

An attempt has been made to determine the extent to which the intact structure influences the shear strength by normalizing the shearing data for volume, thereby deriving the state boundary surface. An intrinsic state boundary surface (SBS*) is usually obtained using the isotropic normal compression line (NCL*) as a reference. However, the choice of normalising with respect to critical state line (CSL*) was necessary due to difficulties in clearly identifying NCL*s. This is because high pressures would be required and there were difficulties in testing the samples at such high pressures due to equipment limitations and membrane puncture.

The stress paths of the reconstituted and intact samples have been normalized by an equivalent pressure taken on the critical state line p'_{cs}, ($p'_{cs} = \exp(\Gamma\text{-}v)/\lambda)$) and the critical state line gradient M. This makes the critical state plot on the coordinate (1:1). Similar to the normalization I_v in compression, one CSL gradient has been assumed but with a different intercept Γ for every test, which was calculated from Figure 18 using the initial v of each test. Figure 19 shows the normalized shearing behaviour for the intact and reconstituted samples. The reconstituted stress paths are represented by grey lines, intact samples are represented by black lines and the critical states are represented by black symbols. The intrinsic state boundary surface (SBS*) is represented by short broken line and the intact SBS depicted by long broken line. The size of the intact SBS is larger than intrinsic SBS* on the wet side indicating the effects of structure, similar to behaviour in compression, although with a complete convergence to the same critical state that the reconstituted soil would have at that initial specific volume. As discussed above the isotropic compression paths for the reconstituted soils may not have been taken to high enough pressures to be sure of identifying accurately the wet side of the SBS*. However, from the comparison of the isotropic compression behaviour of intact and reconstituted samples on Fig. 17 there is a very clear difference in Group 3 for intact and reconstituted samples of similar initial specific volumes, with the intact sample that was loaded to the highest stresses clearly reaching states further to the right of the CSL* than the reconstituted samples at similar stresses. It does not seem that loading to still higher pressures would change this, confirming that the SBS* is significantly smaller than the intact SBS.

Conclusions

The mechanics of a transitional mode of behaviour in a decomposed volcanic rock have been investigated by carrying out oedometer and triaxial tests on intact and reconstituted samples. The behaviour is characterised by parallel normal compression and critical state lines that highlight the transitional mode of behaviour in both compression and shearing, particularly for the reconstituted samples. For the intact samples, the difficulty of having only a narrow range of initial (in-situ) specific volumes and also too few tests in these difficult soils meant that the pattern is less clear. This is, however, the first time that any transitional behaviour has been identified in a weathered soil from an igneous rock.

Using the factors m and P proposed by Ponzoni et al. (2014) to quantify transitional behaviour, the m value for compression is significantly less than the P value for shear. From m the soil can be classified as having a medium transitional behaviour, but using the locations of the CSLs (P), the value for the decomposed volcanic rock is higher than other published values. A robust fabric that is difficult to break down is likely to be the cause of the transitional behaviour, and comparisons with a CDV of similar grading but conventional non-transitional behaviour did highlight very different fabrics. It was interesting that there were significant differences between the behaviour of the intact and reconstituted soil, which must also be the result of other elements of structure.

Allowing for the influence of the initial specific volume through normalisation, showed that these elements of structure were much less broken down by compression than shear, and so are rather different to those causing the transitional behaviour. Identifying which elements of structure cause differences between the intact and reconstituted soil and which cause transitional behaviour remains a challenge for future research. Since it is difficult for practising engineers to observe the soil fabrics with routine laboratory testing equipment, properties of these type of materials can be only be characterised completely by considering the non-uniqueness of their normal compression and critical state lines. However, providing that good intact samples are tested our engineering design parameters, such as angle of shearing resistance or compressibility, will still be valid for design in the soils in-situ even if conventional tests and analysis would not allow us to understand the role of structure.

Acknowledgements

This work was supported by a grant from the Research Grant Council of the Hong Kong Special Administrative Region (HKSAR), China (T22-306/15N). The authors would like to thank Mr Sunny So of the Civil Engineering and Development Department (CEDD) of HKSAR for the assistance in obtaining the samples used for this work.

Notations

The following symbols are used in this paper:

C_u = coefficient of uniformity;

d_{50} = mean particle size;

e = void ratio;

e^*_{100} = void ratios at 100kPa;

e^*_{1000} = void ratios at 1000kPa;

I_v = void index;

p' = mean normal effective stress;

p'_{cs} = equivalent pressure taken on CSL;

p'_0 = mean effective stress prior to shearing;

v = specific volume;

Γ = intercept of the CSL at 1kPa; and

λ = gradient of the NCL or CSL.

References

Burland JB (1990) On the compressibility and shear strength of natural clays. Geotechnique 40(3):329-378.

Cotecchia F (1996). The effects of structure on the properties of an Italian Pleistocene clay. University of London, Ph.D Thesis.

Ferreira PMV, Bica AVD (2006) Problems on identification of the effects of structure and critical state in a soil with a transitional behaviour. Geotechnique 56(7):445-454.

Geotechnical Engineering Office (1988) Guide to rock and soil descriptions, Geoguide 3. Geotechnical Engineering Office, Civil Engineering Dept., Government of the Hong Kong SAR.

ISRM (2007) The Complete ISRM Suggested Methods for Rock Characterization, Testing and Monitoring [1974–2006]. In: Ulusay, R., Hudson, J. (Eds.*)*, International Society of Rock Mechanics.

Martins F, Bressani LA, Coop MR, Bica VD (2001) Some aspects of the compressibility behaviour of a clayey sand. Canadian Geotech. J., 38(6):1177-1186.

Nocilla A, Coop MR, Colleselli F (2006) The Mechanics of an Italian Silt; an Example of "Transitional" Behaviour. Geotechnique 56(4):261-271.

Okewale IA (2017). Geotechnical and geological characterisation of decomposed volcanic rocks from Hong Kong. City University of Hong Kong, Ph.D Thesis.

Okewale IA, Coop MR (2017). A study of the effects of weathering on soils derived from decomposed volcanic rocks. Engineering Geology, 222:53-71.

Okewale IA, Coop MR (2018a) On the effects of weathering on the compression behaviour of decomposed volcanic rocks. TuniRock 2018, Hammamet, Tunisia, 85-90.

Okewale IA, Coop MR (2018b) Suitability of different approaches for analysing and predicting the behaviour of decomposed volcanic rocks. Journal of Geotechnical and Geoenvironmental Engineering, 144(9), 1-14.

Okewale IA (2019a) Influence of fines on the compression behaviour of decomposed volcanic rocks. International journal of Geo-Engineering 10(4):1-17.

Okewale IA (2019b) Effects of weathering on the stiffness characteristics and the small strain behaviour of decomposed volcanic rocks. Journal of GeoEngineering, 14(2):97-107.

Okewale IA (2019c) On the intrinsic behaviour of decomposed volcanic rocks. Bull Eng. Geol. and the Env., 1-12.

Okewale IA (2020) Applicability of chemical indices to characterize weathering degrees in decomposed volcanic rocks. Catena, 189:1-13.

Okewale IA, Grobler H (2020) A study of dynamic shear modulus and breakage of decomposed volcanic soils. J. GeoEng. 15(1):55-68.

Ponzoni E, Nocilla A, Coop MR (2017) The behaviour of a gap graded sand with mixed mineralogy. Soils and Foundations 57:1030-1044.

Ponzoni E, Nocilla A, Coop MR, Colleselli, F (2014) Identification and quantification of transitional modes of behaviour in sediments of Venice lagoon. Geotechnique 64(9):694-708.

Rocchi I, Coop MR (2014) Experimental accuracy of the initial specific volume. Geotechnical Testing J. 37(1):169–175.

Rocchi I, Okewale IA, Coop MR (2015) The behaviour of Hong Kong volcanic saprolites in one-dimensional compression. Volcanic Rocks and Soils: Rotterdam: Balkema. 281-287.

Rocchi I, Coop MR (2015) The effects of weathering on the physical and mechanical properties of a granitic saprolite. Geotechnique 65(6):482-493.

Rocchi I, Coop MR (2016) Mechanisms of compression in well-graded saprolitic soils. Bull Eng Geol Environ.

Shipton B, Coop MR, Nocilla A (2006) Particle breakage in transitional soils. Geomechanics and Geotechnics of Particulate Media, Taylor and Francis Group, London, 143-147.

Shipton B, Coop MR (2012) On the compression behaviour of reconstituted soils. Soils and Foundations, 52(4):668-681.

Shipton B, Coop MR (2015) Transitional behaviour in plastic and non-plastic soils. Soils and Foundations, 55(1):1–16.

Todisco MC, Coop MR, Perreira J-M (2018) Fabric Characterisation in transitional soils. Granular Matter, 20(20):1-12.

Xu L, Coop MR (2017) The mechanics of a saturated silty loess with a transitional mode. Geotechnique, 67(7):581-596.

Figure captions

Fig 1 Grading curves of the samples

Fig 2 Micrographs of the intact samples

Fig 3 Micrographs of the reconstituted samples

Fig 4 One-dimensional compression behaviour for the reconstituted samples

Fig 5 One-dimensional compression for the reconstituted CDV samples (Okewale and Coop, 2017)

Fig 6 SEM images showing fabric of the CDV samples; (a) reconstituted and (b) intact (Okewale and Coop, 2017)

Fig 7 One-dimensional compression for the intact samples

Fig 8 One-dimensional compression for the intact CDV samples (Okewale and Coop, 2017)

Fig 9 Calculation of degree of convergence in compression for the samples

Fig 10 Normalised compression behaviour using void index I_v

Fig 11 Stress-strain behaviour for undrained triaxial tests of the reconstituted and intact samples; (a) q:ε_a, and (b) $\Delta u/p'_o$

Fig 12 Stress-strain behaviour for drained triaxial tests of the reconstituted and intact samples; (a) q:ε_a, and (b) ε_v:ε_a

Fig 13 Stress paths and critical states for the samples

Fig 14 Evolution of stress ratios for the samples

Fig 15 Non-convergence of states in drained shearing

Fig 16 Non-convergence of states in undrained shearing

Fig 17 Behaviour of the samples in volumetric plane; (a) reconstituted and (b) intact and reconstituted

Fig 18 Calculations of P value for the samples

Fig 19 Normalised shear behaviour for the samples

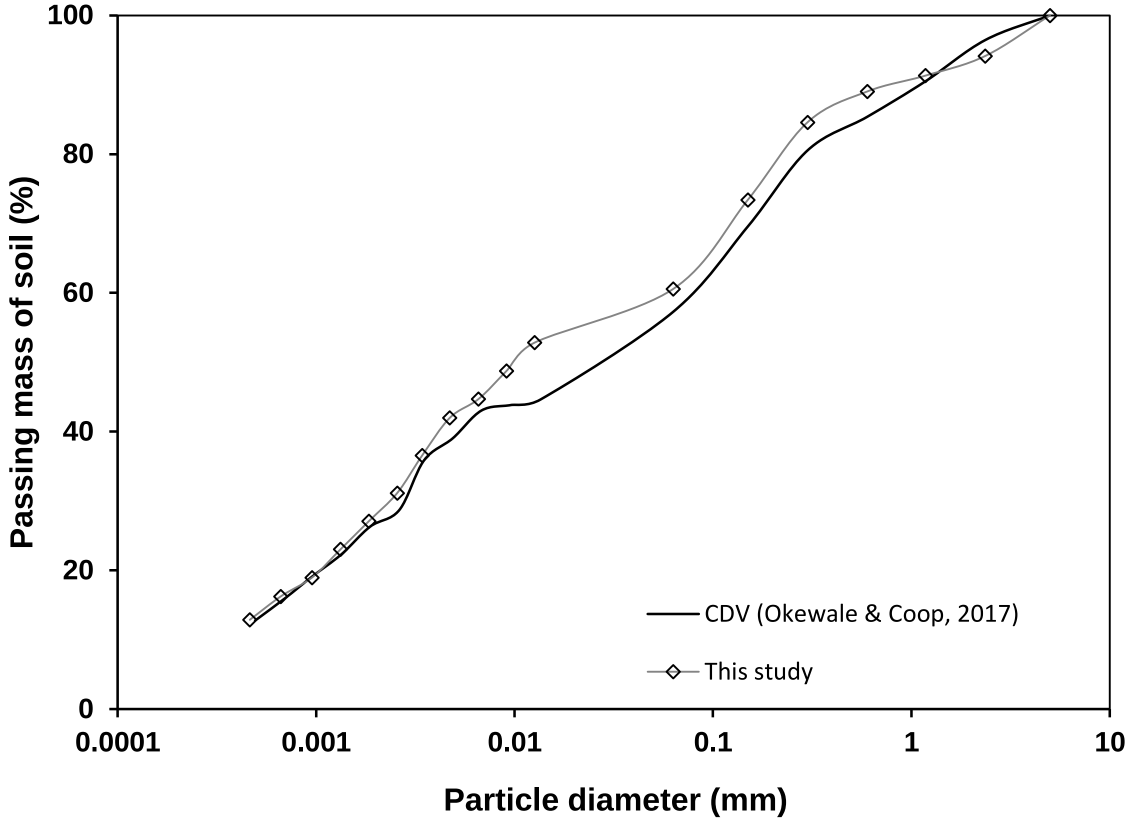

Fig 1 Grading curves of the samples

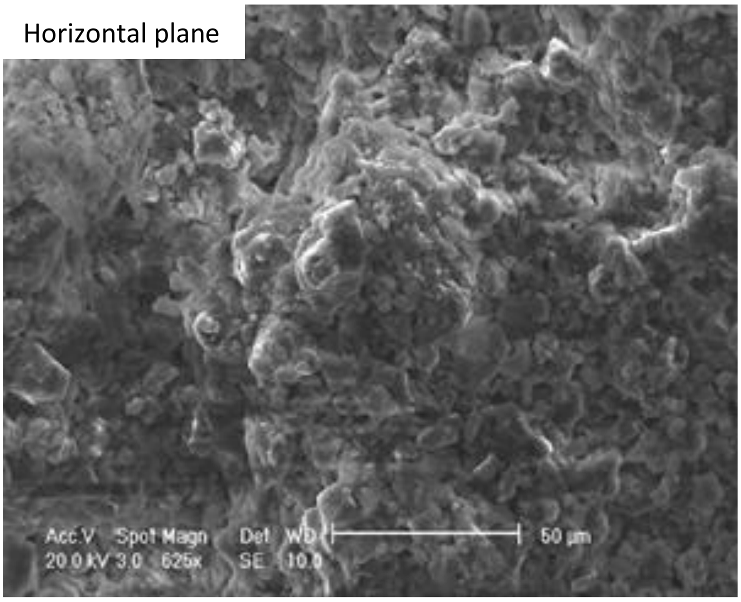

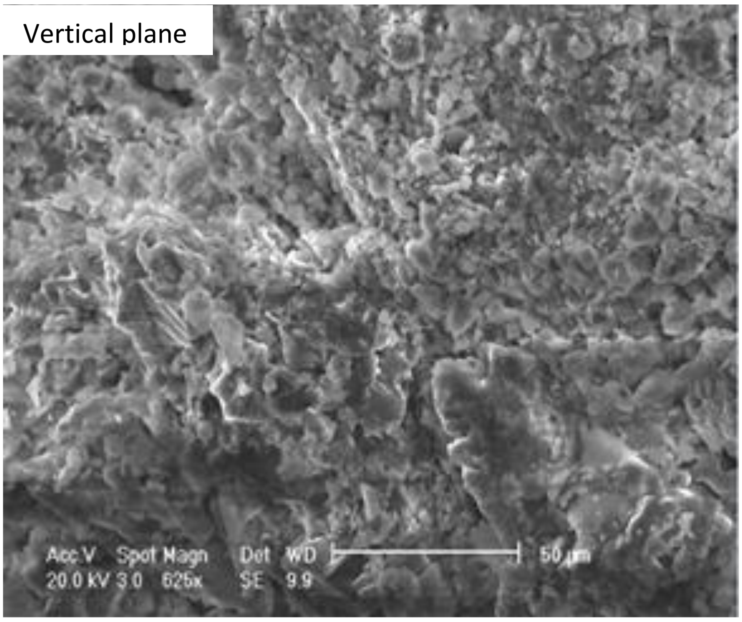

Fig 2 Micrographs of the intact samples

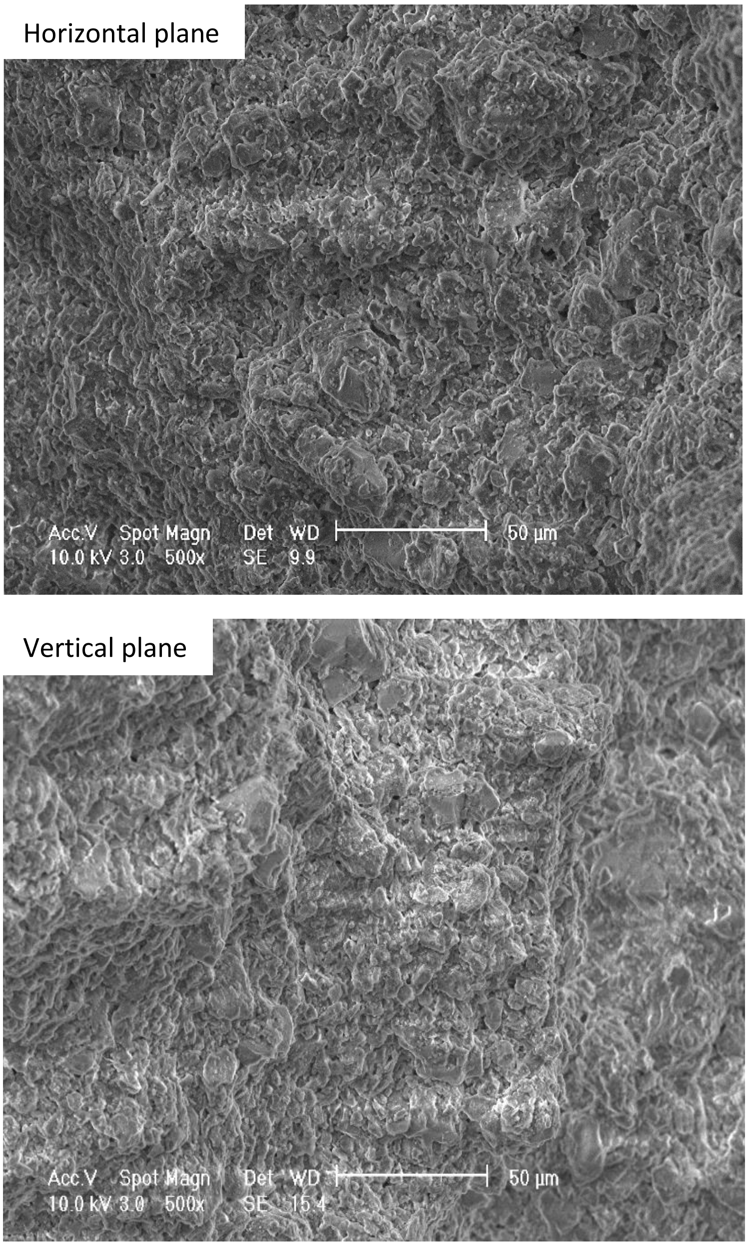

Fig 3 Micrographs of the reconstituted samples

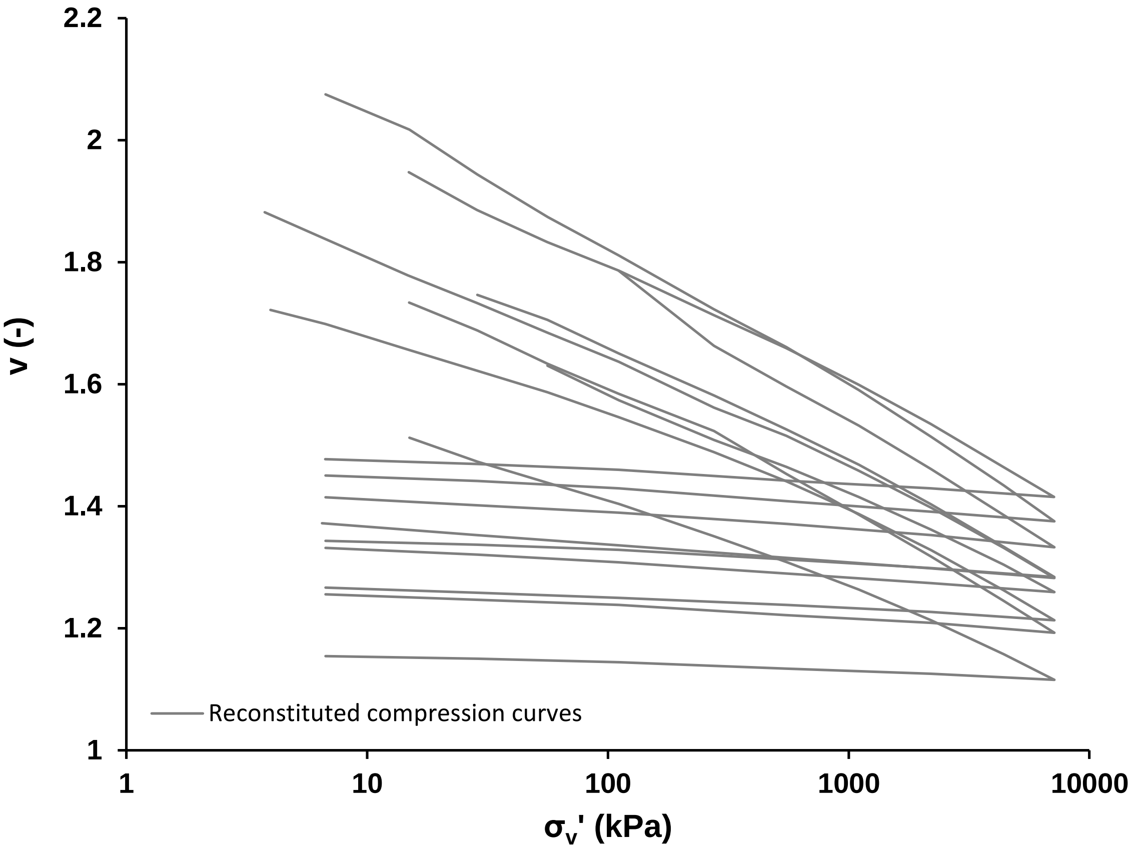

Fig 4 One-dimensional compression behaviour for the reconstituted samples

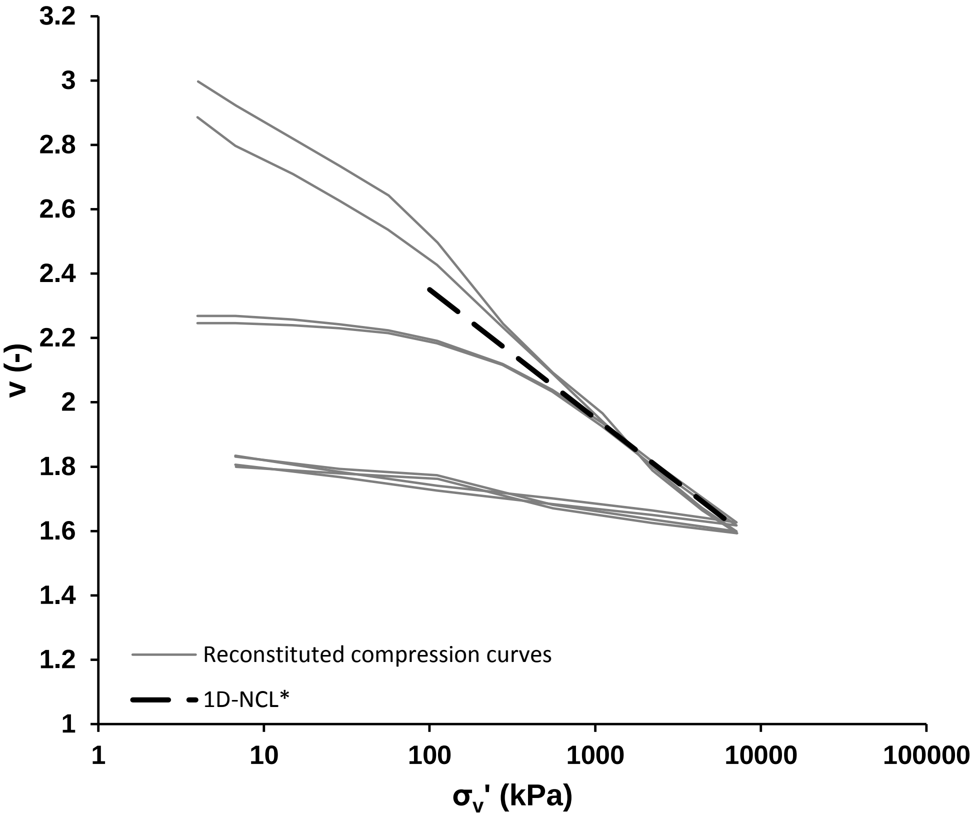

Fig 5 One-dimensional compression for the reconstituted CDV samples (Okewale and Coop, 2017)

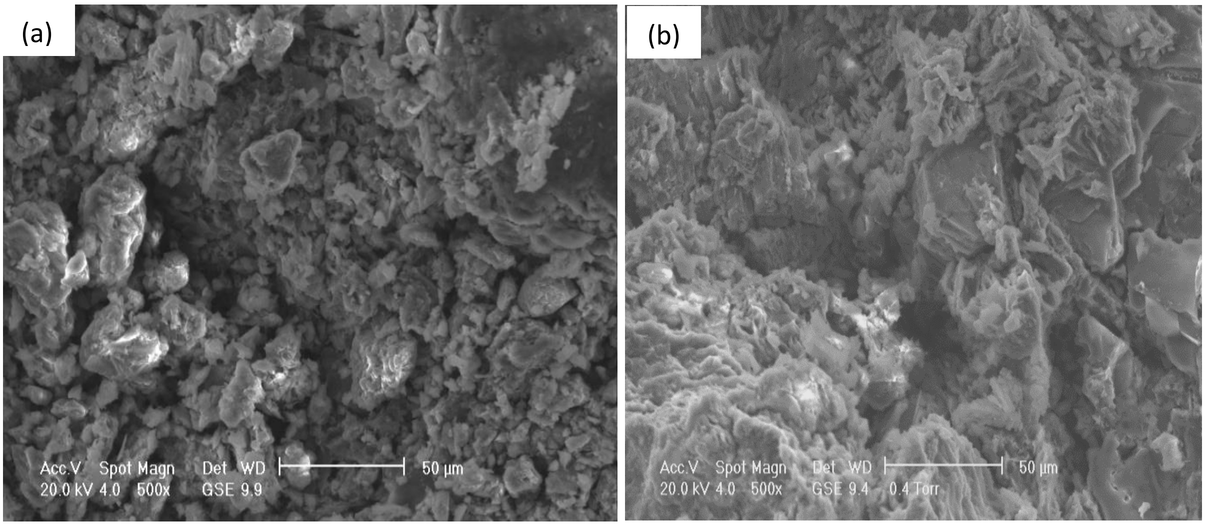

Fig 6 SEM images showing fabric of the CDV samples; (a) reconstituted and (b) intact (Okewale and Coop, 2017)

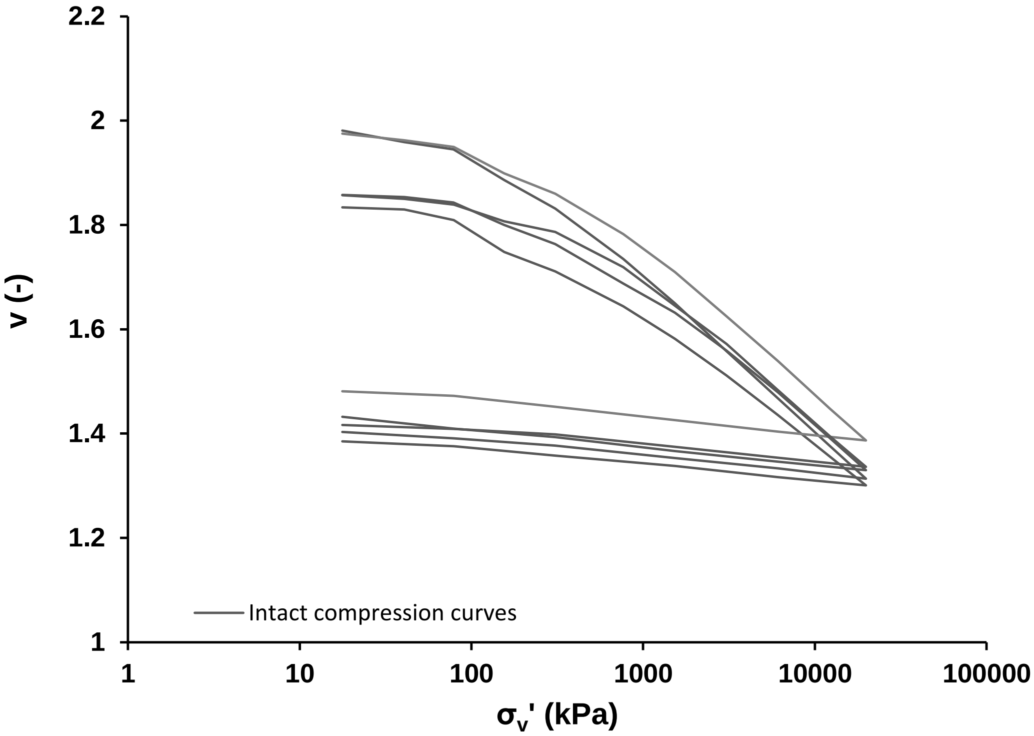

Fig 7 One-dimensional compression for the intact samples

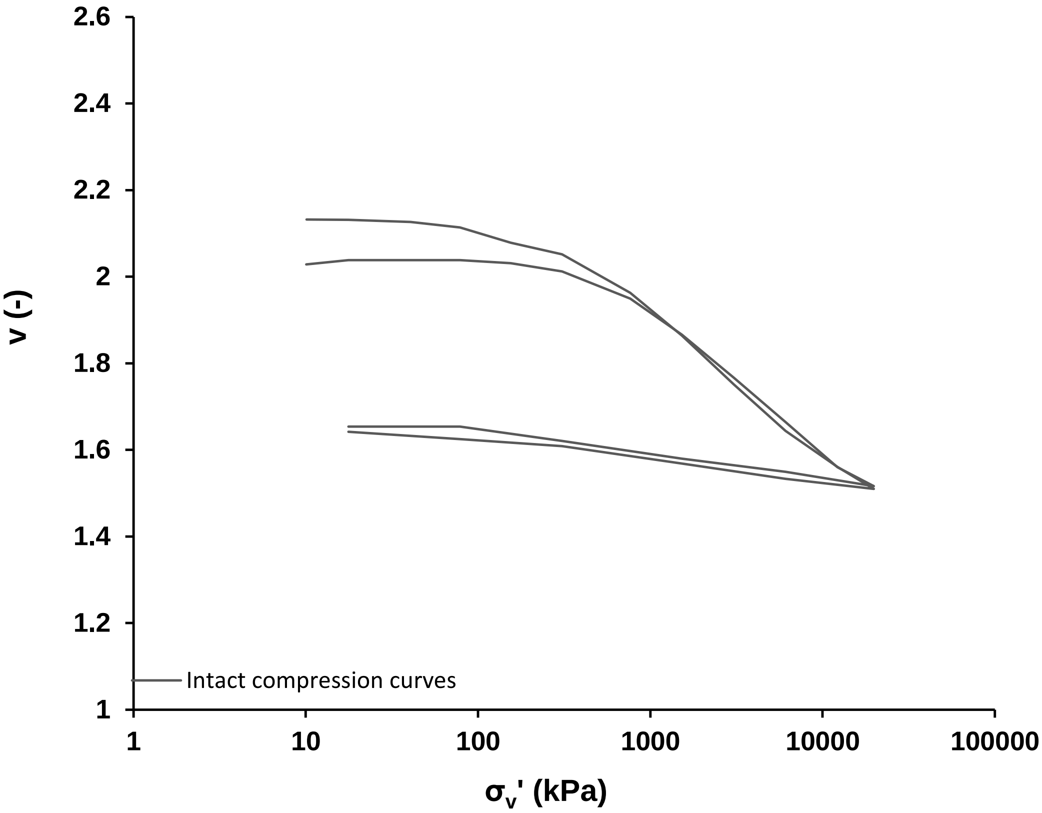

Fig 8 One-dimensional compression for the intact CDV samples (Okewale and Coop, 2017)

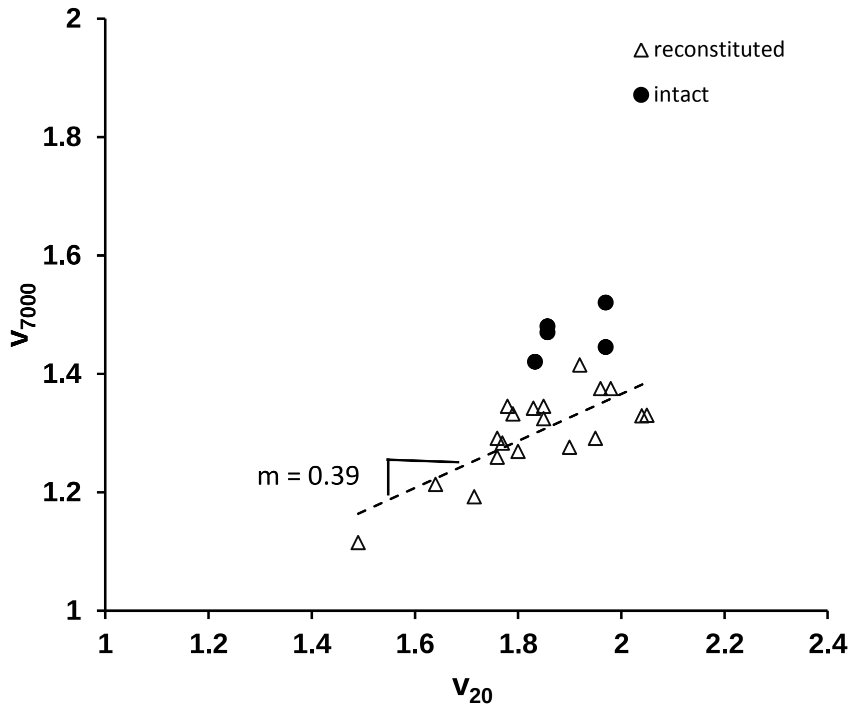

Fig 9 Calculation of degree of convergence in compression for the samples

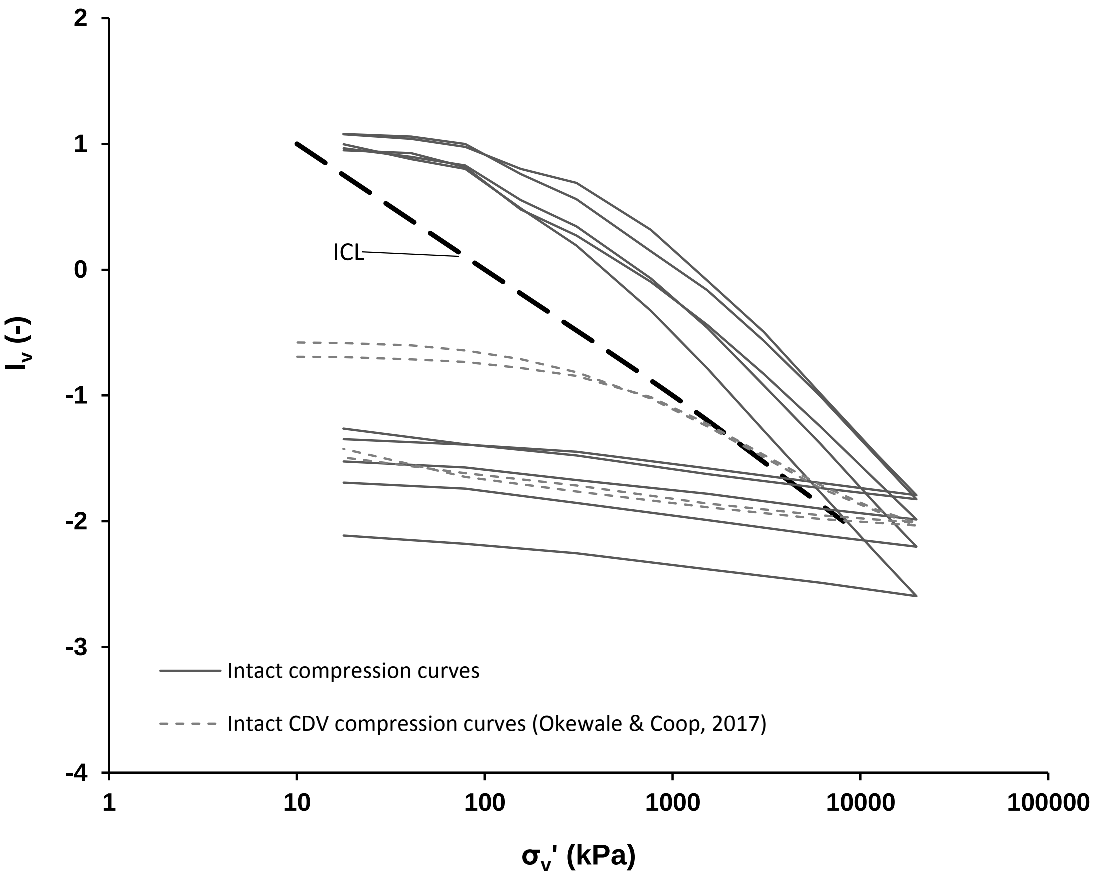

Fig 10 Normalised compression behaviour using void index I_v

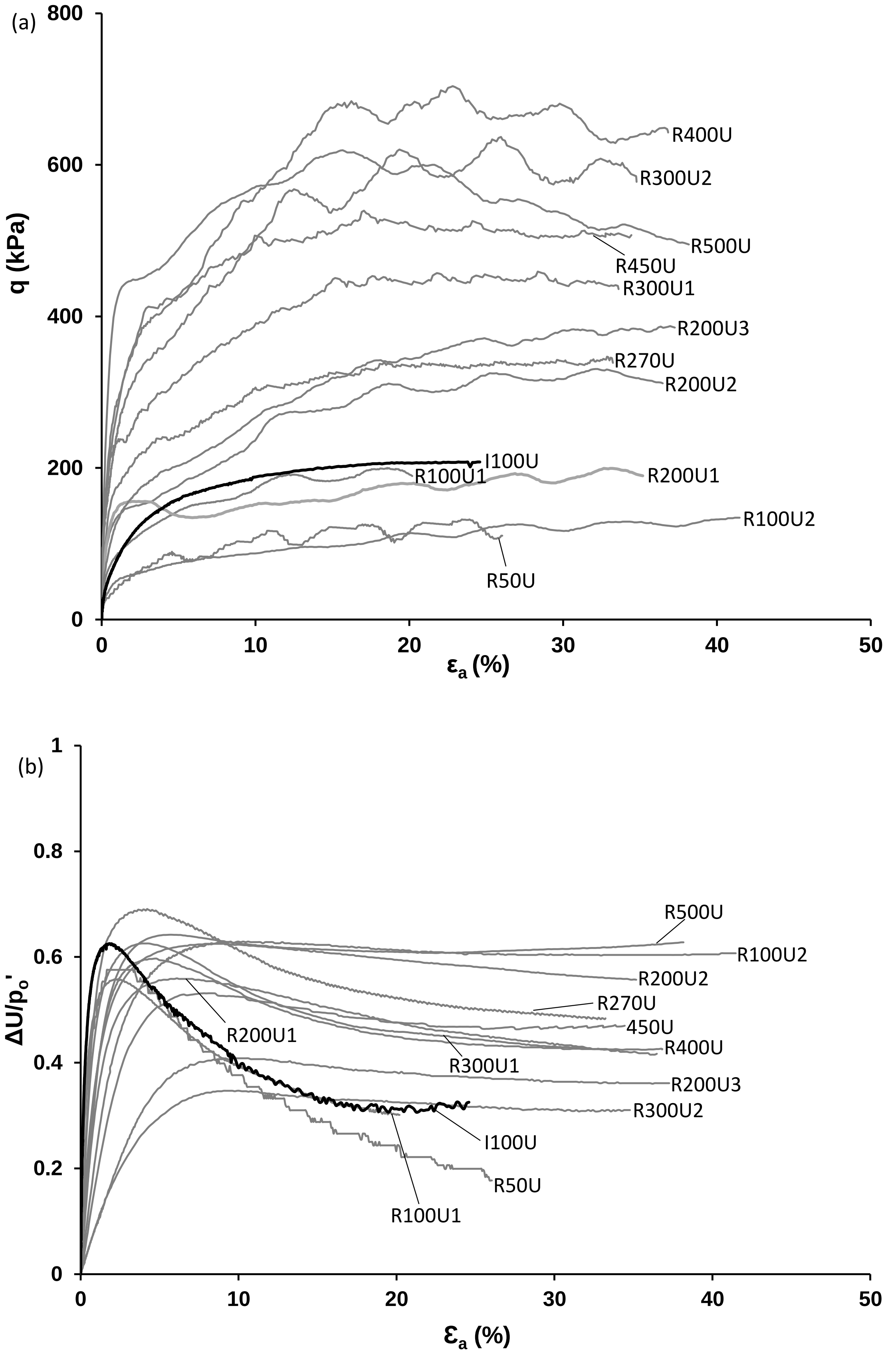

Fig 11 Stress-strain behaviour for undrained triaxial tests of the reconstituted and intact samples; (a) q:ε_a, and (b) $\Delta u/p'_o$

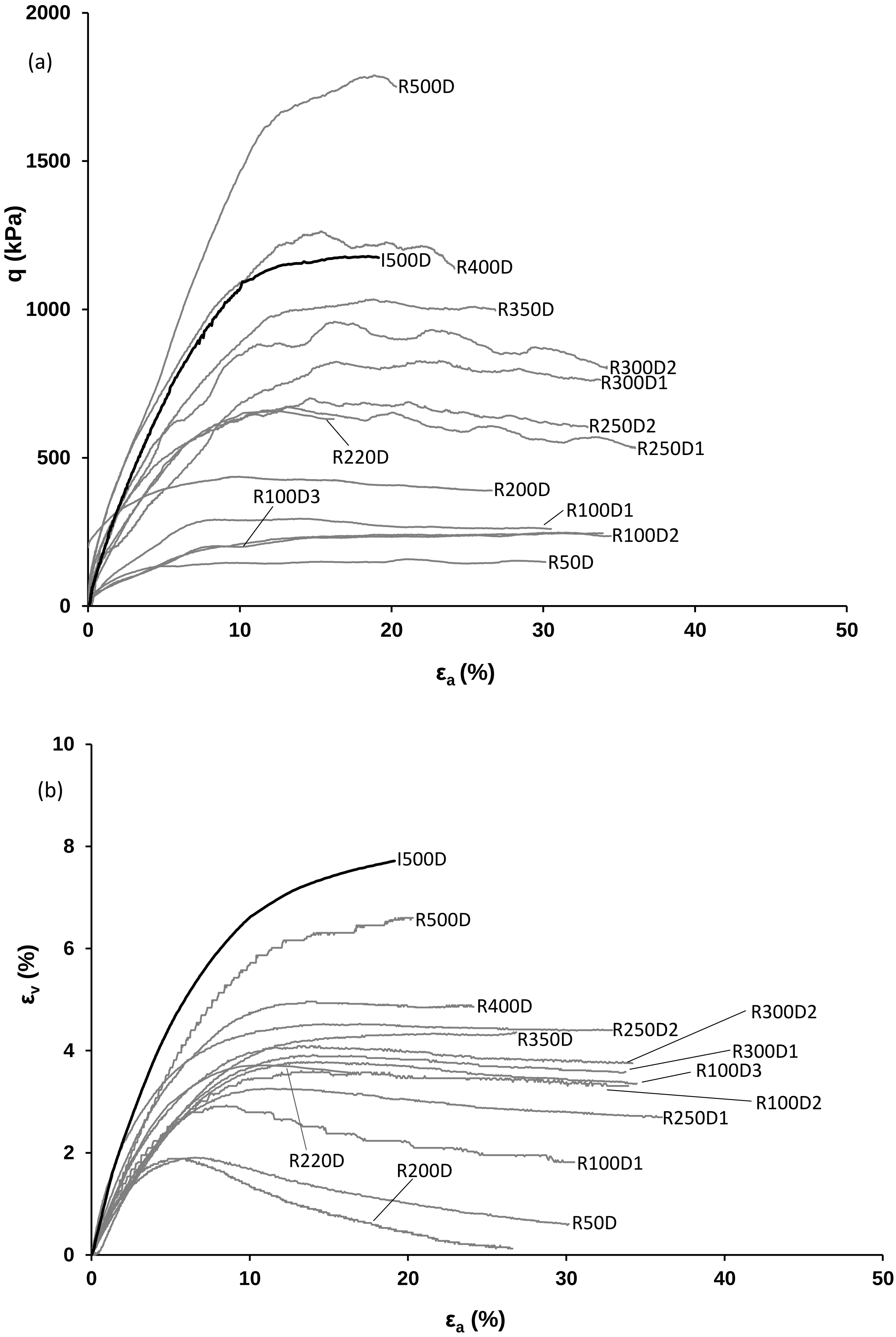

Fig 12 Stress-strain behaviour for drained triaxial tests of the reconstituted and intact samples; (a) q:ε_a, and (b) ε_v:ε_a

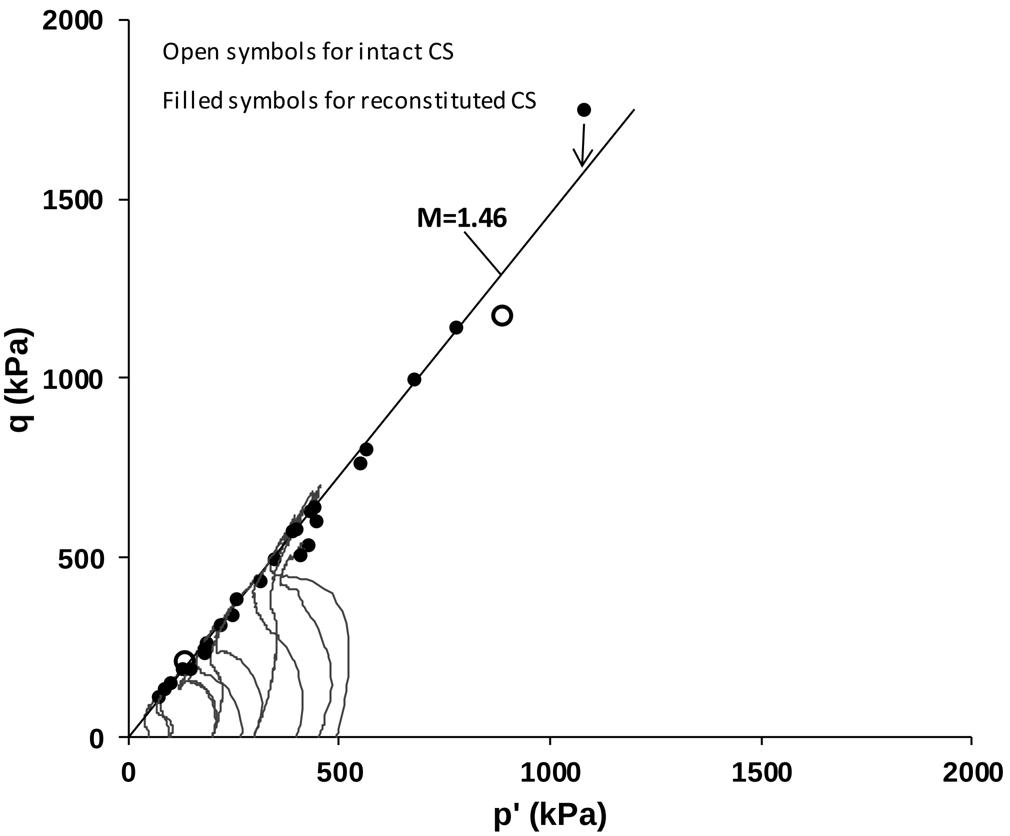

Fig 13 Stress paths and critical states for the samples

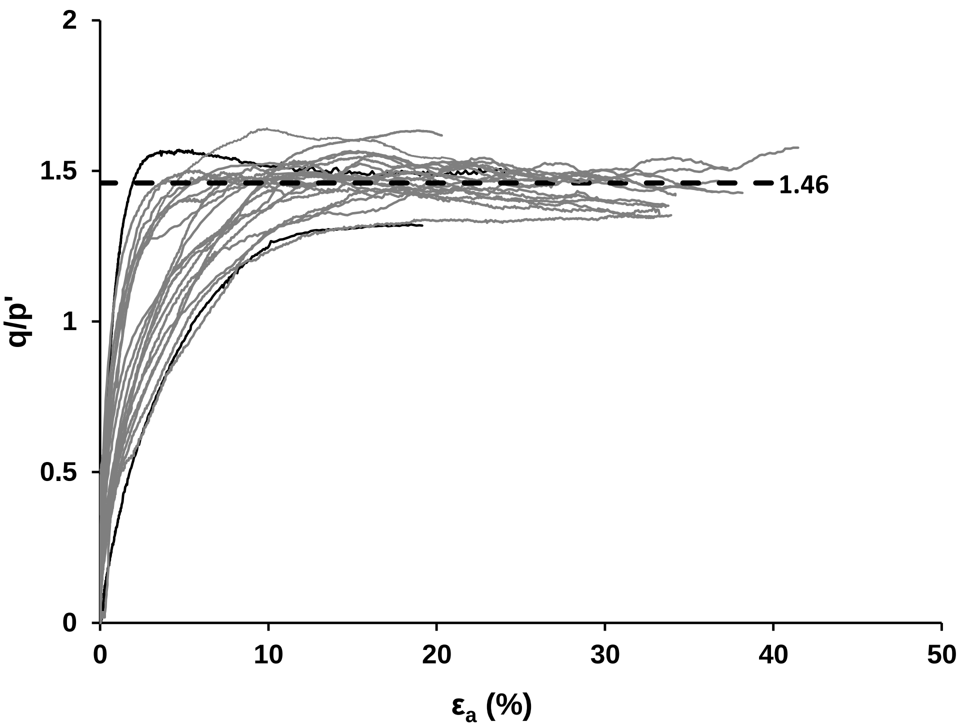

Fig 14 Evolution of stress ratios for the samples

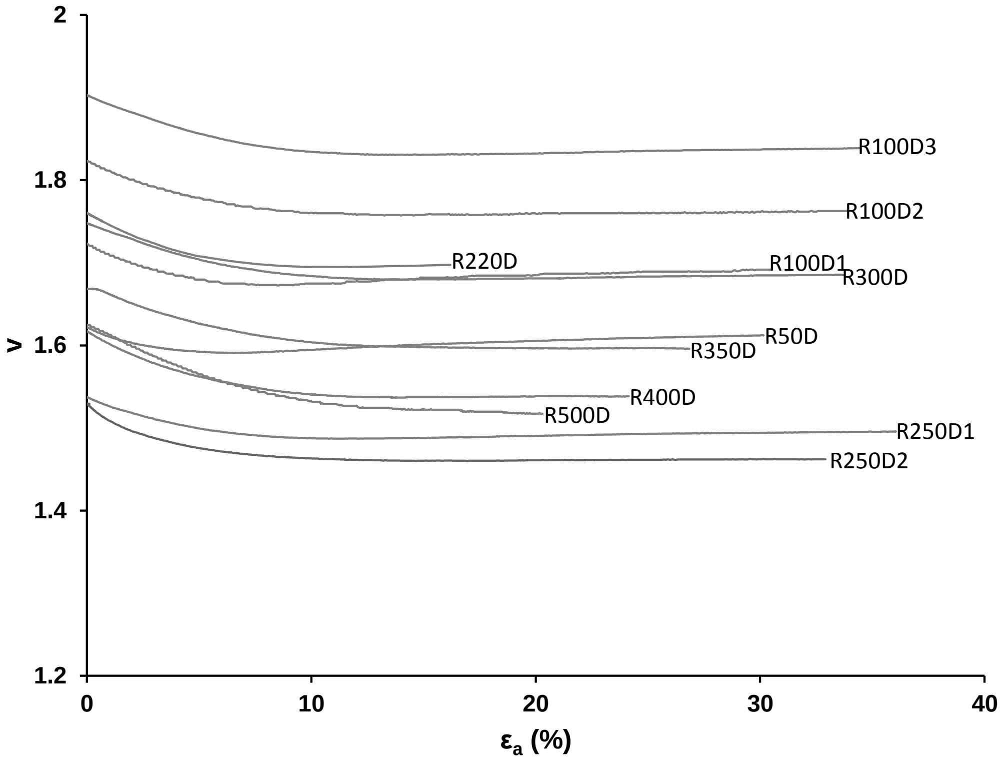

Fig 15 Non-convergence of states in drained shearing

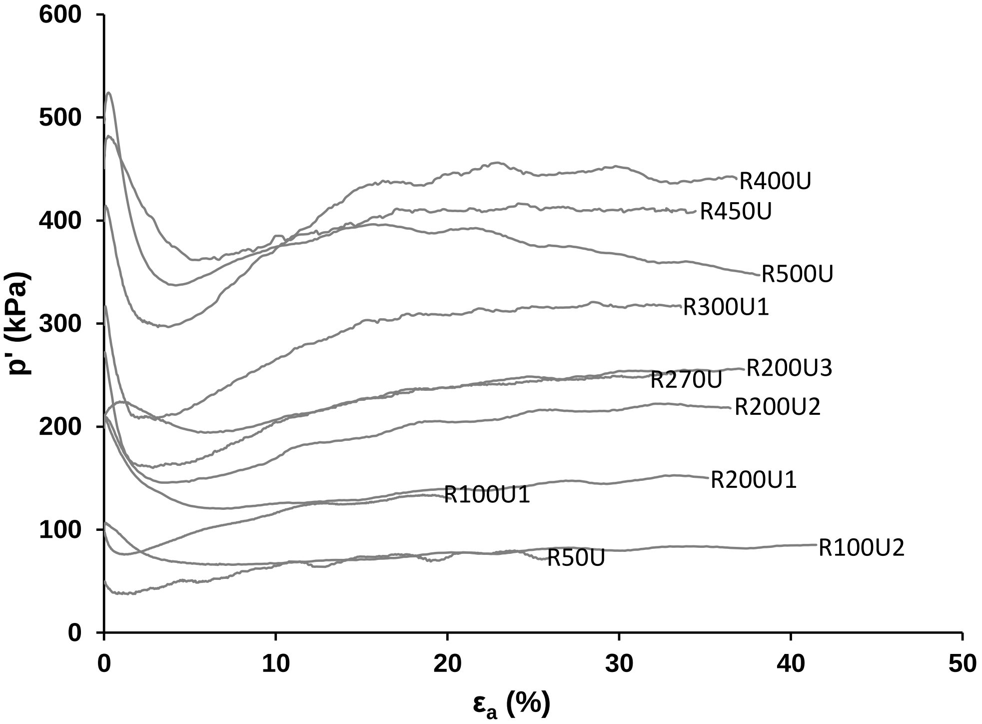

Fig 16 Non-convergence of states in undrained shearing

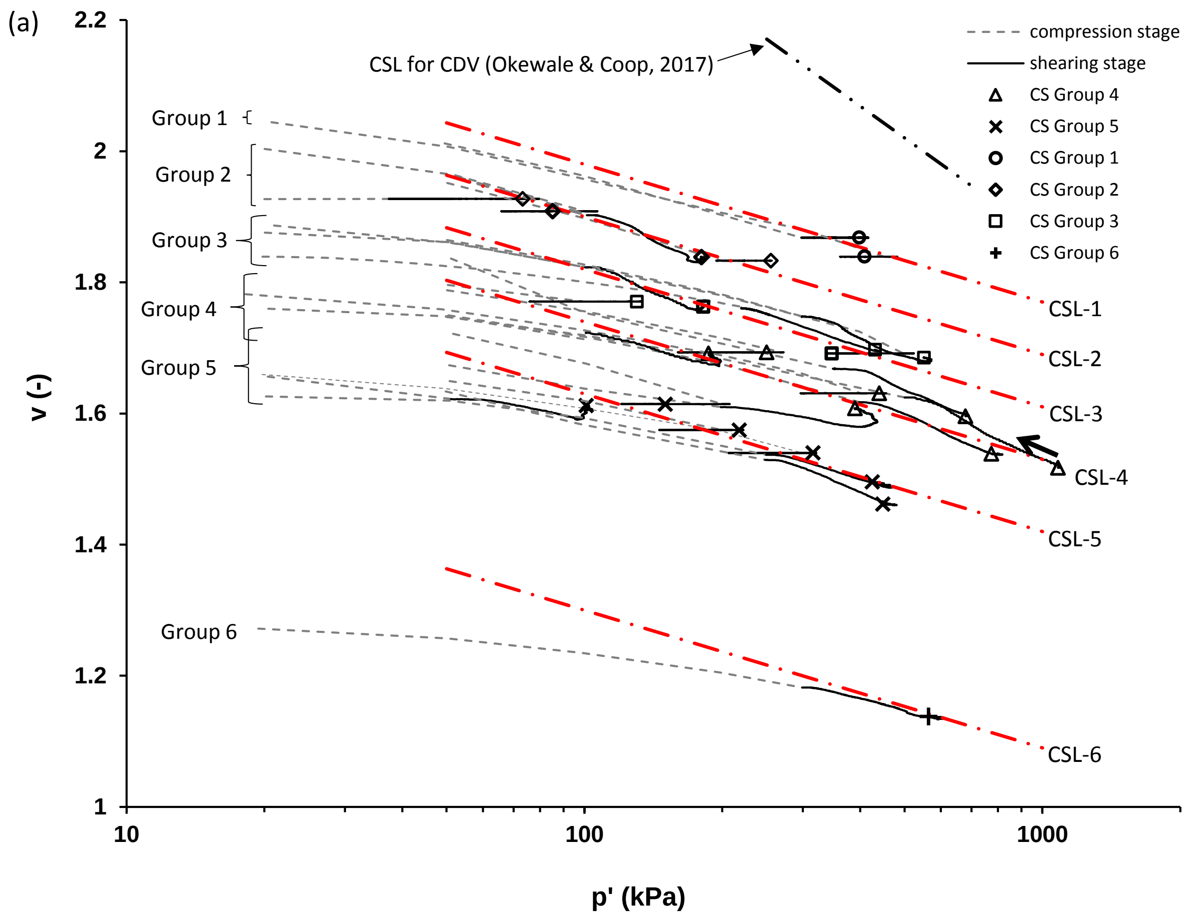
(a)
CSL for CDV (Okewale & Coop, 2017)
compression stage
shearing stage
CS Group 4
CS Group 5
CS Group 1
CS Group 2
CS Group 3
CS Group 6
Group 1
Group 2
Group 3
Group 4
Group 5
Group 6
CSL-1
CSL-2
CSL-3
CSL-4
CSL-5
CSL-6
v (-)
p' (kPa)
2.2
2
1.8
1.6
1.4
1.2
1
10
100
1000

546

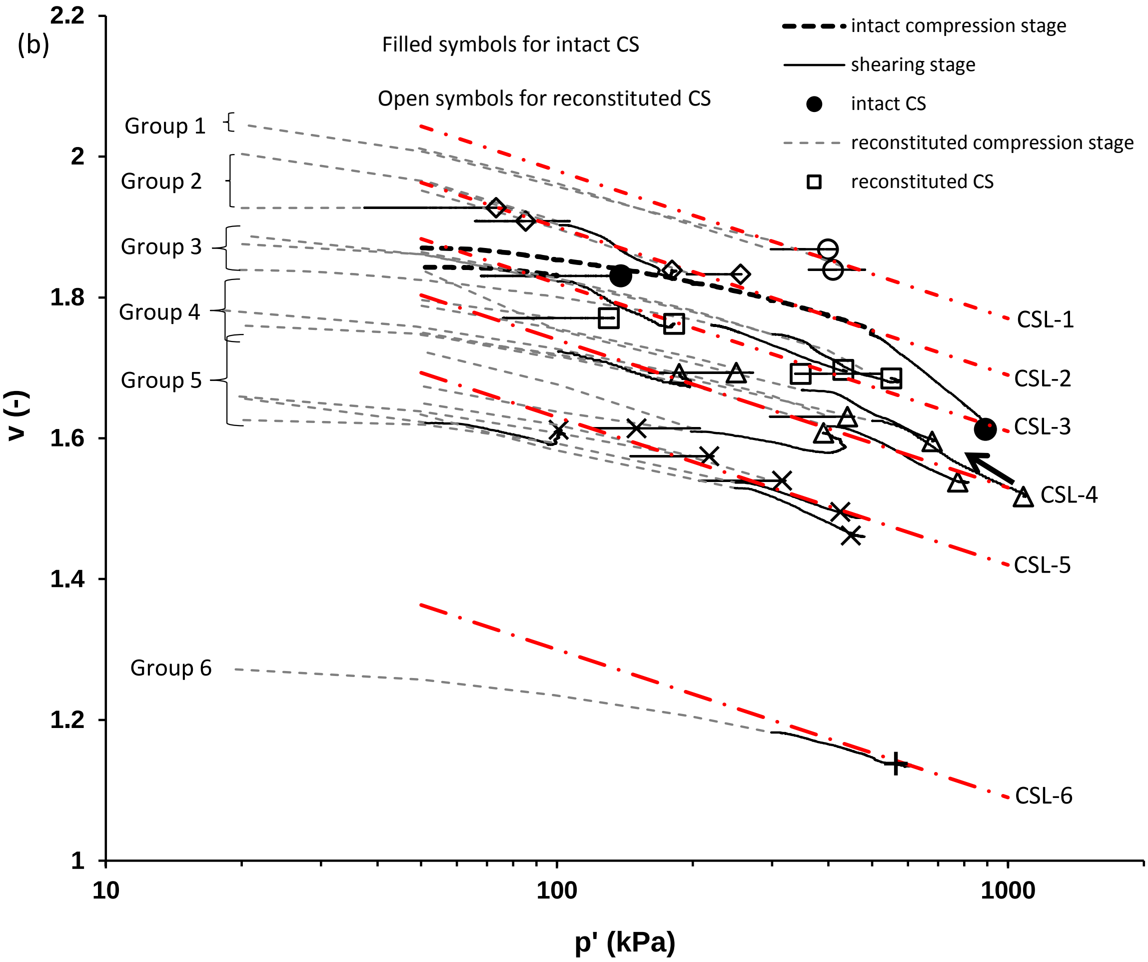

Fig 17 Behaviour of the samples in volumetric plane; (a) reconstituted and (b) intact and reconstituted

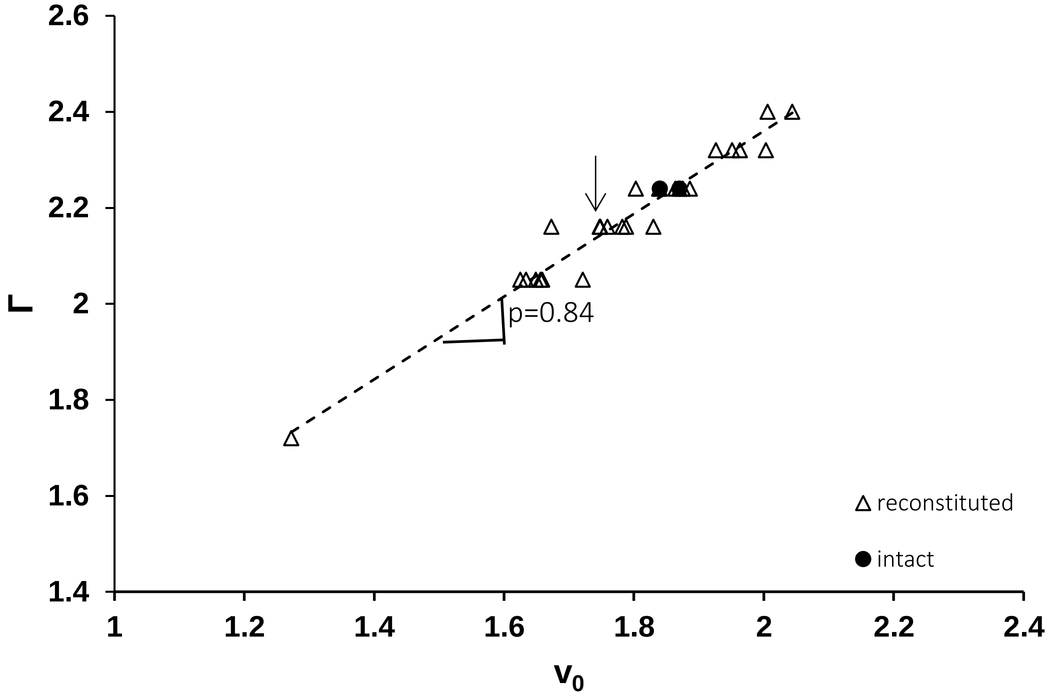

Fig 18 Calculations of P value for the samples

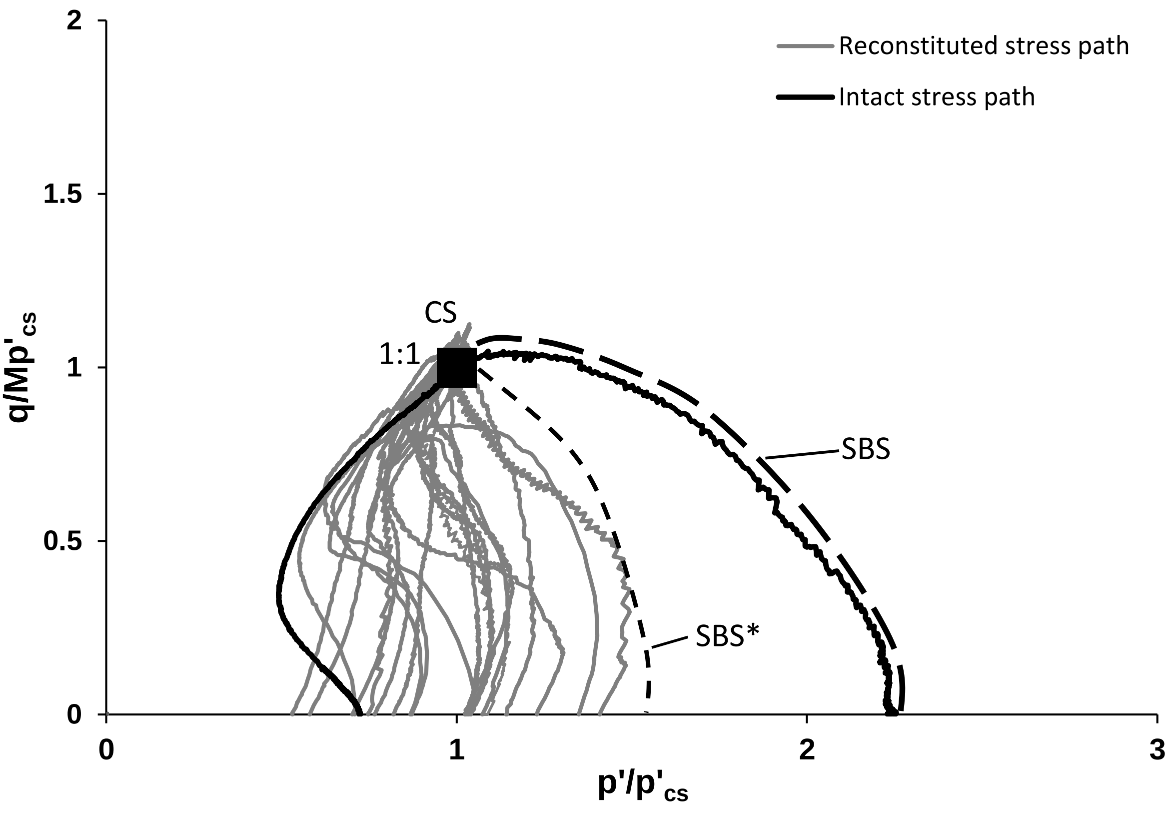

Fig 19 Normalised shear behaviour for the samples

Table 1. Sample description and index properties

Formation	Depth (m)	Grading	d_{50} (mm)	c_u	Clay Fraction (%)	Silt Fraction (%)	Liquid limit (%)	Plastic limit (%)	Plasticity index (%)
TMSF	4-5	Coarse	0.01	150	28	30.7	35.5	26.1	9.4

TMSF Tai Mo Shan Formation, d_{50} mean particle size, c_u coefficient of uniformity

Table 2. Mineralogy from XRD analysis

Minerals (%)			
Quartz	Feldspars	Clays	Others
37	20	30	13

Table 3. Chemical compositions from XRF analysis

Chemical compositions (%)							
Na_2O	CaO	MgO	Al_2O_3	SiO_2	K_2O	TiO_2	Fe_2O_3
1.44	0.27	0.06	19.42	62.14	2.23	1.54	12.90

Table 4. Details of oedometer tests

Sample/test type	w_i	v_i	$\sigma_{v\ max}$ (kPa)
RO1	0.275	1.787	7145
RO2	0.499	2.304	7155
RO3	0.419	2.093	7152
RO4	0.447	2.192	7124
RO5	0.422	2.144	7144
RO6	0.306	2.319	7147
RO7	0.409	2.137	7147
RO8	0.420	2.126	7141
RO9	0.418	2.126	7152
RO10	0.444	2.002	7158
RO11	0.407	2.019	7144
RO12	0.470	2.254	7144
RO13	0.459	2.152	7139
RO14	0.323	1.907	7138
RO15	0.323	1.893	7151
RO16	0.359	2.008	7165
RO17	0.362	2.002	7171
RO18	0.390	2.017	7171
RO19	0.530	2.390	7165
IO1	0.320	1.991	19854
IO2	0.273	1.992	19854
IO3	0.273	1.839	19854
IO4	0.302	1.861	19854
IO5	0.327	1.858	19854

R reconstituted, I intact, w_i initial/ in-situ water content, v_i initial specific volume, $\sigma_{v\ max}$ maximum vertical stress.

Table 5. Details of triaxial tests

Sample/test type	v_i	p'_c (kPa)	v_c	End of shearing		
				q_{cs} (kPa)	p'_{cs} (kPa)	v_f
R50U	1.940	48	1.927	110	73	1.927
R50D	1.656	50	1.622	148	100	1.612
R100U1	1.800	100	1.770	189	130	1.770
R100U2	2.000	100	1.908	134	85	1.908
R100D1	1.759	100	1.712	260	186	1.691
R100D2	1.875	100	1.822	245	181	1.762
R100D3	2.006	100	1.902	236	180	1.838
R200U1	1.649	199	1.574	311	217	1.574
R200U2	1.721	199	1.631	189	150	1.631
R200U3	1.983	199	1.832	385	255	1.832
R200D	1.673	198	1.609	630	407	1.607
R220D	1.839	219	1.760	630	430	1.697
R250D1	1.625	249	1.537	531	425	1.495
R250D2	1.633	248	1.529	602	448	1.461
R270U	1.805	269	1.693	338	249	1.693
R300U1	1.659	299	1.539	435	315	1.539
R300U2	2.046	298	1.868	577	398	1.868
R300D1	1.875	299	1.747	762	551	1.685
R300D2	1.271	299	1.182	800	564	1.137
R350D	1.836	349	1.668	995	679	1.595
R400U	1.781	399	1.631	642	440	1.631
R400D	1.774	399	1.616	1239	809	1.538
R450U	2.044	450	1.839	507	409	1.839
R500U	1.886	497	1.691	495	346	1.691
R500D	1.768	500	1.624	1750	1081	1.517
I100U	1.842	98	1.830	207	138	1.830
I500D	1.870	500	1.747	1174	890	1.612

R reconstituted, I intact, v_i initial specific volume, p'_c mean effective stress prior to shearing, v_c specific volume before shearing, q_{cs} deviatoric stress at critical state, p'_{cs} mean effective stress at critical state, v_f final specific volume.